

Dust in Protoplanetary Disks

E. I. Chiang

UC Berkeley Astronomy, 601 Campbell Hall, Berkeley CA 94720

Abstract. We critically examine the best lines of evidence for grain growth in protoplanetary disks, based on modelling of observed spectral energy distributions and images of T Tauri and Herbig Ae stars. The data are consistent with millimeter-sized grains near disk midplanes, and micron-sized grains near disk surfaces. We review three channels by which grains can grow, including direct condensation from the vapor phase, grain-grain collisional sticking, and gravitational instability. The utility of dust in identifying as yet unseen extrasolar planets is highlighted.

1. Introduction

By studying dust in disks surrounding pre-main-sequence stars, we believe we glimpse the progenitors of planets. In this review, we ask three questions: What is the observational evidence for grain growth in circumstellar, presumably protoplanetary disks? What is our theoretical understanding of how grains grow from the submicron sizes that typify grains in the diffuse interstellar medium (ISM) to the kilometer-sized planetesimals that furnish the building blocks of planets? And finally, how can we use dust to trace the presence of extrasolar planets?

2. Observational Evidence for Grain Growth

2.1. Models

Interpretation of emission from grains in disks relies on models for how radiation is transferred through disks. The simplest models to consider are passive; the disk derives its luminosity by re-processing incident light from the central star. Models of passive disks in radiative and hydrostatic equilibrium are constructed by Chiang & Goldreich (1997, hereafter CG97) and Chiang et al. (2001, hereafter C01). The models assume that dust dominates the broadband opacity of the disk from optical to millimeter wavelengths. We examine in Figures 1 and 2, respectively, a schematic of how radiation is transferred in externally irradiated disks, and a sample spectral energy distribution (SED). We distinguish two contributions to the emission above the Rayleigh-Jeans tail of the stellar blackbody. At wavelengths, λ , of a few microns to $\sim 60 \mu\text{m}$, emission arises from the hot, “superheated” surface layers of the disk. By definition, grains in these surface layers directly intercept radiation from the central star; these naked grains are heated to temperatures above that of blackbody if their sizes,

a , are smaller than the wavelengths characteristic of the re-emitted radiation. For the emissivities of bare silicates and ice-coated silicates employed by C01, surface grain temperatures are typically $3 \times$ that of blackbody; for this reason, we refer to these grains as “superheated.”¹ These hot grains radiate their heat more or less isotropically. Half of their thermal emission immediately escapes into space, where Earth-bound astronomers perceive it to arise from an optically thin medium. The other half is directed downwards into the deeper disk interior for further reprocessing. The models of CG97 and C01 crudely treat the interior as an isothermal (not necessarily optically thick) slab. The contribution to the SED from the disk interior, which at a given stellocentric distance, r , is cooler than the disk surface by a factor of ~ 3 , is marked by the dashed line in Figure 2. It dominates at $\lambda \gtrsim 100 \mu\text{m}$. For more sophisticated treatments of radiative transfer that spatially resolve the disk interior, see Calvet et al. (1991), D’Alessio et al. (1998), and Dullemond, van Zadelhoff, & Natta (2002).

The assumption of passivity is well justified since disks tend to be geometrically flared; the pressure scale height of passively reprocessing disks scales as $h \propto r^\gamma$, where $\gamma > 1$. To the extent that the height of the superheated surface layer, H , follows h , the concavity of the disk surface enables the disk to intercept more stellar energy at a given r than is locally released by accretion.² For this inequality to hold, a rule of thumb is that H must exceed the radius of the central star. For typical T Tauri parameters, passive reprocessing of starlight dominates the local energy budget at $r \gtrsim 0.5 \text{ AU}$ or, equivalently, at $\lambda \gtrsim 10 \mu\text{m}$. The point is not that the disk is not actively accreting; most T Tauri and Herbig Ae stars do evince ultraviolet (UV) excesses and veiling at optical wavelengths that betray accretion in their immediate vicinity; the point instead is that one would be hard pressed to tell whether a disk is accreting based on the infrared (IR) SED alone. The insensitivity of the infrared SED to the physics of disk accretion is a bane to those who wish to understand the transport of mass and momentum at large stellocentric distances, and a boon to those who wish to model SEDs and infer disk temperatures, gas densities, and grain sizes.

By assuming that dust dominates the opacity in circumstellar disks, we are saying that the forest of lines contributed by circumstellar molecules such as H_2 , CO, and H_2O cover a small fraction of the continuum spectrum longward of $\sim 10 \mu\text{m}$. This is likely a fine assumption at $r \gtrsim 1 \text{ AU}$, where gas densities are typically so low (a consequence of the weak tidal gravity field of the star) that molecular lines should be thermally broadened and therefore narrow (CG97). Closer to the star, pressure broadening may render this assumption problematic. A careful accounting of gas chemistry and opacity in the centralmost disk should be performed. If recent explanations (e.g., Dullemond, Dominik, & Natta 2001) of the near-IR excesses of Herbig Ae stars in terms of central AU-sized cavities are to be believed, such an accounting had better yield gas disks that are optically thin.

¹Not to be confused with the phenomenon of temperature spiking of $a \lesssim 0.01 \mu\text{m}$ grains in the ultraviolet radiation field of the diffuse ISM.

²If dust and gas are well-mixed in cosmic proportions, then H/h varies from 5 to 4 across the entire disk, which spans $\sim 10^2 \text{ AU}$ (C01).

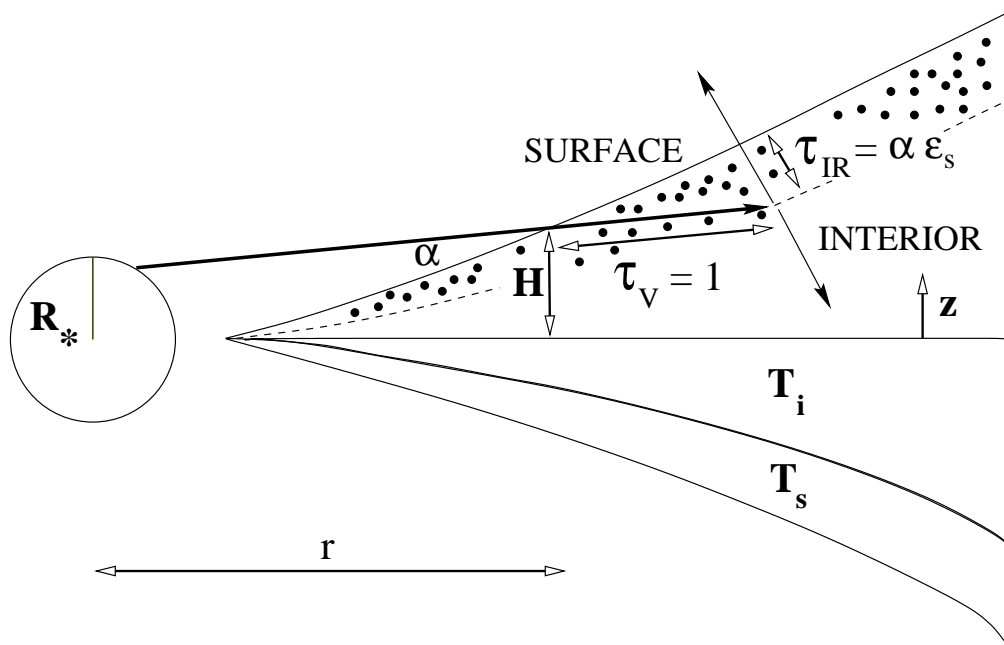


Figure 1. Schematic of radiative transfer in passively reprocessing circumstellar disks. The disk surface layer is defined as containing grains that first intercept radiation from the central star. Surface grains radiate their heat isotropically; roughly half of the reprocessed radiation immediately escapes into space, while the other half is directed downwards into the disk interior for further reprocessing. The height of the disk surface is geometrically flared and enables the disk to reprocess substantially more starlight at a fixed stellocentric distance than an actively accreting disk would. For details and an explanation of the various variables, see Chiang & Goldreich (1997), from which this figure was taken.

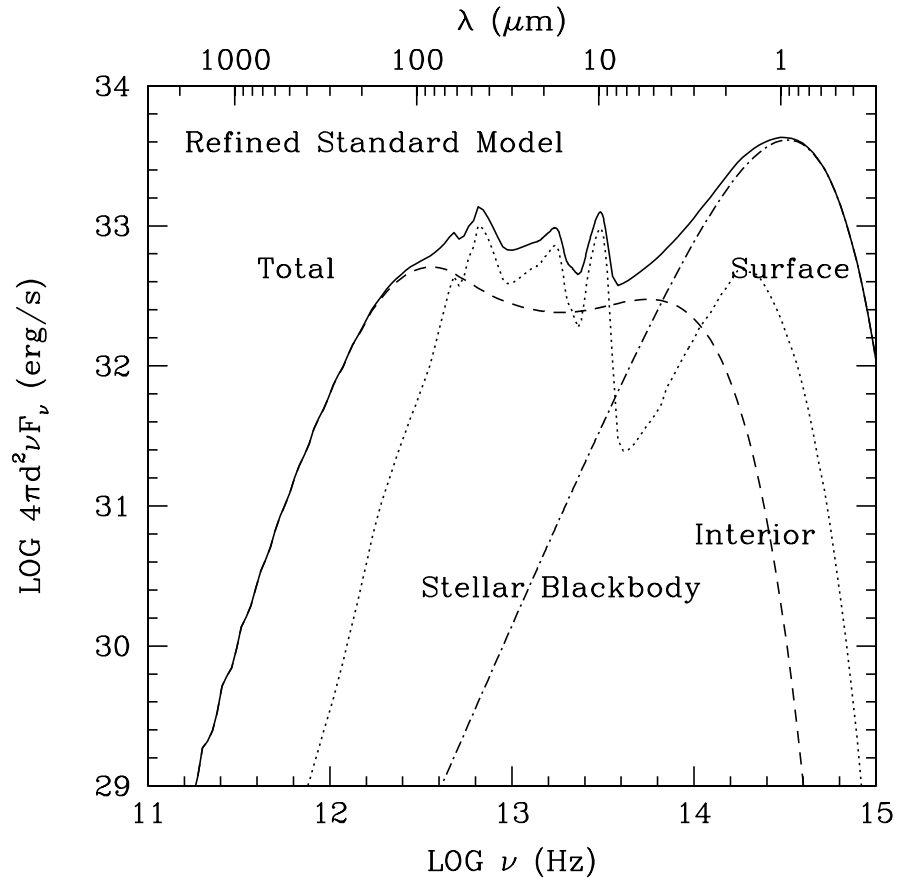


Figure 2. Sample SED of a passive disk from Chiang et al. (2001). The central star contributes the blackbody spectrum peaked at $1 \mu\text{m}$. Disk emission can be divided into two parts, one from the surface layers that dominate the flux at mid-infrared wavelengths, and a second from the cooler disk interior that dominates at $\lambda \gtrsim 100 \mu\text{m}$. Surface grains are composed of amorphous olivine and crystalline water ice; hence the solid-state emission bands at $\lambda \sim 10, 18, 45,$ and $60 \mu\text{m}$.

The main purpose of this subsection has been to provide a theoretical backdrop against which to interpret observations of disks. From Figures 1 and 2, we recognize that thermal emission at mid-infrared wavelengths probes the hot exterior skins of disks. Emission at millimeter wavelengths probes conditions closer to the cooler disk midplane. And scattered (optical-to-IR) light measurements necessarily implicate disk surfaces. We proceed to examine critically the best lines of evidence for grain growth that observations and modelling currently offer.

2.2. Grain Growth in the Disk Interior: Millimeter-wave Emission

Claims of grain growth in T Tauri and Herbig Ae disks have been based on the slope of the SED at millimeter wavelengths (e.g., Koerner, Chandler, & Sargent 1995); it is tempting to take the common observation that $\delta \equiv d \log F_\nu / d \log \nu < 4$ to imply that $\beta \equiv d \log \kappa_\nu / d \log \nu = \delta - 2 < 2$, where κ_ν is the opacity and ν is the frequency of observation. In the diffuse ISM where particle sizes do not approach ~ 1 mm, β takes its value in the Rayleigh limit of 2. Values smaller than 2 are held as evidence for grain growth to millimeter sizes; in the geometric optics limit, $\beta \approx 0$.

The problem with such reasoning is that it assumes the disk is optically thin at wavelengths where the spectral slope is measured. Emission from an optically thick medium would give $d \log F_\nu / d \log \nu = 2$ and a spurious inference that $\beta \approx 0$. Such issues were appreciated by early and ground-breaking millimeter-wave studies of pre-main-sequence stars (Beckwith et al. 1990; Beckwith & Sargent 1991); the review by Beckwith, Henning, & Nakagawa (2000) carefully outlines the assumptions and caveats behind conclusions based purely on measured spectral slopes. To address the concern of contamination by emission from optically thick media, we must turn to detailed modelling of disks. Chiang et al. (2001) fit the IR-to-mm wavelength SEDs of 4 Herbig Ae stars and 1 T Tauri star using a more sophisticated version of the 2-layer model of CG97.³ They account for grain size distributions and employ laboratory-measured optical constants of silicates and water ice. In every pre-main-sequence system, the mm-wave SED is consistent with grain size distributions for which the mass is concentrated in mm-sized particles. Grains are modelled as (possibly ice-mantled) spheres in C01; this simplification is not expected to be particularly restrictive; Henning & Stognienko (1996) compute opacities of fluffy, fractal aggregates and find values similar to those of compact spheres. Unless grains are dominated by highly conductive materials such as iron, grain shape is not expected to alter opacities by more than factors of a few.

Despite this remarkable news that pre-main-sequence circumstellar disks may be awash in sand-sized particles, these detailed modelling efforts serve also to accentuate the severe degeneracies involved in fitting SEDs. Figure 3, taken from C01, illustrates this degeneracy; the same dataset can be fitted with either a small-mass disk containing large grains or a large-mass disk containing small grains. The degeneracy reflects the fact that the flux, F_ν , from an optically

³In particular, they correct a faulty estimate of CG97 that κ_ν , the opacity of the dust-gas mixture at visible wavelengths, is of order $400 \text{ cm}^2/\text{g}$. A more realistic estimate is closer to $3 \text{ cm}^2/\text{g}$.

thin medium scales as its optical depth, $\tau_\nu = \Sigma\kappa_\nu$, where Σ is the disk surface density. One measurement of $F_\nu \leftrightarrow \tau_\nu$ cannot break the degeneracy between Σ (disk mass) and κ_ν (grain size).⁴

We are aware of one pre-main-sequence system for which this degeneracy is tantalizingly close to being broken. That system is TW Hydra, a 8 Myr-old T Tauri star that sports a beautiful, face-on circumstellar disk and is a mere 56 pc away. Weinberger et al. (2002) and Calvet et al. (2002) both model the SED and find the grain mass distribution to be weighted towards centimeter-sized grains. Calvet et al. (2002) proceed further to show that their SED-based solution for the disk is consistent with the spatially resolved mm-wave continuum images of the TW Hya disk. What is particularly intriguing about these large grain-size solutions is that, if one further assumes that gas and dust are mixed in cosmic proportions of $\Sigma_{\text{gas}}/\Sigma_{\text{dust}} \sim 10^2$, then the Toomre Q -parameter of this disk is near unity. Toomre's Q measures the susceptibility of the disk to growth of perturbations by self-gravity. It scales as $Q \propto 1/\Sigma$; values far above unity imply stability, while values far below unity imply violent instability on the local orbital timescale. Discounting the large grain-size solution in favor of smaller grains forces κ_{mm} to decrease and Σ_{gas} to increase, such that Q falls below unity. This is a recipe for violent gravitational instability that we regard as unpalatable (see also Johnson & Gammie 2003). However, this argument hinges on the assumption of a cosmic gas-to-dust ratio; as we shall mention in §3.3, solar metallicities may not characterize disks that are sufficiently quiescent for dust to drift inwards relative to gas.

2.3. Grain Growth in the Surface Layer: Mid-IR Emission

Silicate emission bands at $\lambda \sim 10 \mu\text{m}$ and $\sim 20 \mu\text{m}$, routinely observed in the spectra of T Tauri and Herbig Ae stars, imply that grains in hot disk surface layers are emitting in the Rayleigh limit, $a \lesssim \lambda/2\pi \sim 2 \mu\text{m}$. The emission band at $\lambda \sim 10 \mu\text{m}$ for TW Hya is spectrally well resolved and constitutes a blend of two features, one centered at $9.6 \mu\text{m}$ due to the Si-O stretching mode in glassy pyroxene, and another at $11.2 \mu\text{m}$ due to the same vibrational mode in crystalline olivine (Weinberger et al. 2002, and references therein). Though crystalline silicates are occasionally evinced in spectra of pre-main-sequence stars (Malfait et al. 1998), most systems exhibit predominantly amorphous silicates. Natta, Meyer, & Beckwith (2000) present $\sim 10 \mu\text{m}$ emission band spectra of nine classical T Tauri stars and reproduce them either with $a \approx 0.1 \mu\text{m}$ grains composed of glassy olivine (30%) and glassy pyroxene (70%), or $a \approx 1 \mu\text{m}$ grains composed purely of glassy pyroxene. Thus, a different degeneracy afflicts inferences of grain growth in the optically thin surface layers: the degeneracy between grain size and grain composition. Large grains exhibit broader emission bands, but then so, too, do small grains having mixed mineralogies.

⁴In principle, further uncertainty exists in determining whether the observed emission arises from a circumstellar disk at all; SEDs of spherical dusty envelopes can be tuned to match SEDs of disks. This degeneracy in the spatial distribution of dust can be broken by imaging. In this review, all systems for which imaging data exist, either at optical or millimeter wavelengths, are seen to be circumstellar disks.

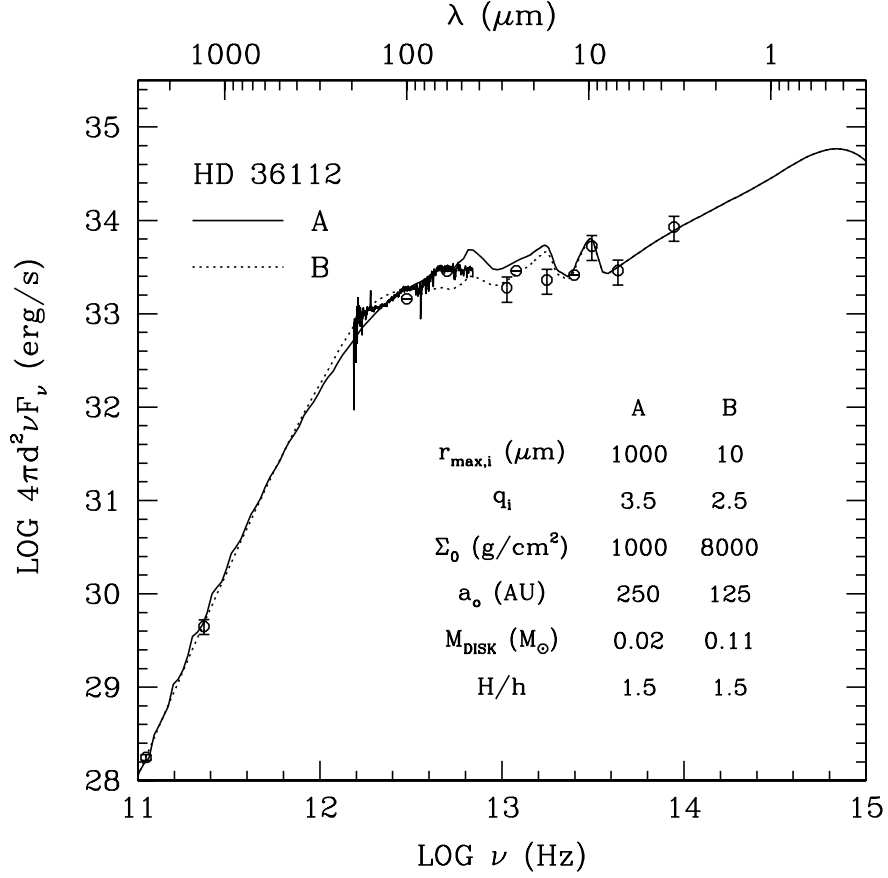


Figure 3. Either a small-mass disk filled with large grains (model A) and or a large-mass disk filled with small grains (model B) can fit the SED of this Herbig Ae star. The disk mass (in gas and dust, mixed in cosmic proportions) is given by M_{DISK} , the maximum size grain in the disk interior is given by $r_{\max,i}$, and q_i is the power-law index for the differential size distribution of grains in the disk interior. For other symbols and a more in-depth discussion, see Chiang et al. (2001), from which this figure was taken.

This degeneracy has recently been showing signs of strain. Van Boekel et al. (2003) report a trend, exhibited by more than 10 Herbig stars, between the strength of the $\sim 10 \mu\text{m}$ feature and its width. The broader the line, the lower is its ratio of peak height to continuum flux. Variations in grain composition alone are argued to be incapable of explaining this trend, since they would change line widths but would affect line strengths less. By contrast, variations in grain size would change both; e.g., if the grain size becomes large enough that the geometric optics limit is reached, then the line would disappear altogether. Thus, the observed trend is most straightforwardly interpreted as an evolutionary sequence of grain sizes; some disks contain $a \approx 1 \mu\text{m}$ -sized grains in their surface layers that produce both weaker and broader emission features than are produced by the $a \approx 0.1 \mu\text{m}$ -sized grains in other disks.

Another breakthrough observation is furnished by McCabe, Duchêne, & Ghez (2003), who present the first spatially resolved image of a T Tauri disk in *scattered* $\lambda \sim 11.8 \mu\text{m}$ light. Keck speckle interferometry proved particularly effective for the opportune viewing geometry of HK Tau B, whose flared disk is oriented at an inclination large enough to extinguish direct (blinding) starlight but small enough to present nearly its full face as a scattering surface. The spatial extent of the reflection nebulosity is ~ 70 AU (full width at half maximum), far too large to be explained by thermal emission from surface grains. The image is reproduced best by employing surface grains having scattering asymmetry parameters of $g \approx 0.15\text{--}0.83$; smaller g -values correspond to nearly isotropic emitters that produce too much flux at large stellocentric distances, while larger g -values generate a nearly unresolved point source.⁵ To the extent that surface grains can be modelled using Mie theory, $0.15 \lesssim g \lesssim 0.83$ corresponds to grain sizes $1.5 \lesssim a(\mu\text{m}) \lesssim 3.2$ (McCabe et al. 2003).

These are not the only examples we can point to for evidence of grain growth in disk surface layers. For example, images of the edge-on disk in HH 30 at various near-infrared wavelengths have led Cotera et al. (2001) and Wood et al. (2002) to conclude that grains at least twice as large as those typifying the maximum size grains in the ISM must be present at altitude; if the unadulterated ISM mix were employed, the variation in extinction with wavelength would be too strong compared with observation.

To summarize these last two subsections, we have seen that the presence of millimeter-sized grains in the dense midplanes of circumstellar disks is certainly consistent with the millimeter-wave spectral and imaging data, though to be fair, the existence of such large grains is not unambiguously demanded. The presence in disk surface layers of amorphous silicate grains having sizes of $0.1\text{--}2 \mu\text{m}$, with an occasional component of crystalline silicates, is on more sure footing. We proceed to describe in broad terms our theoretical understanding of how grains grow.

⁵The g -value is the value of $\cos \theta$ averaged over the power pattern of scattered light, where θ is the angle relative to the direction of the incident beam. See, e.g., Bohren & Huffman (1983), p.72.

3. From Dust to Planetesimals: Theory

We identify three channels for grain growth: accretion from the vapor phase, grain-grain collisional sticking, and gravitational instability.

3.1. Condensation from Vapor

Gas densities at the midplanes of typical models of protoplanetary disks are so high that growth timescales for grains are extremely short compared to the estimated lifetimes of disks. In the standard model of the minimum-mass solar nebula (MMSN) as constructed by CG97, the gas density (H, He, plus solar complement of metals) at the midplane is $\rho_g \sim 10^{-9}(r/\text{AU})^{-39/14}$ g/cm³. A condensation nucleus that accretes metals from the vapor phase increases its radius at the rate of

$$\frac{da}{dt} \sim \frac{Z\rho_g}{\rho_p} c_s \sim 1 \left(\frac{r}{\text{AU}} \right)^{-3} \text{ cm/yr} , \quad (1)$$

independent of the size of the nucleus. Here $Z \sim 10^{-2}$ is the metallicity of the gas, $c_s \approx 0.1 (r/\text{AU})^{-3/14}$ km/s is the sound speed of condensing vapor, and $\rho_p \approx 2$ g/cm³ is the internal density of the grain. Over the lifetime of the disk of $\sim 10^7$ yr, a condensation nucleus can grow to a maximum size of

$$a_{\text{max}} \sim 10^7 \left(\frac{r}{\text{AU}} \right)^{-3} \text{ cm} . \quad (2)$$

Of course, before declaring victory in our effort to grow grains, we must remember that the final size distribution of grains that accrete from the vapor phase depends on the number of seed condensation nuclei. The seed nuclei compete amongst each other for a finite reservoir of metals. In our opinion, trying to estimate the number of seed nuclei at the onset of grain growth is a task not too far removed from trying to count the number of angels on the head of a pin.

3.2. Grain-Grain Sticking

Numerous experiments, both laboratory-based and computer-simulated, have been executed on aggregates of silica monomers (each monomer having $a \approx 1 \mu\text{m}$) to investigate the conditions under which such aggregates stick. Blum & Wurm (2000) find that similar-sized aggregates that collide at relative velocities of less than ~ 0.2 m/s stick with little restructuring of aggregate bonds. Resultant aggregates are highly porous, with large vacuum filling fractions and a fractal geometry (see also Wurm & Blum 1998). At relative velocities approaching ~ 1 m/s, aggregates not only stick but also compactify—the kinetic energy of the collision is diverted towards rearranging bonds between monomers, and the aggregate is strengthened as a consequence. Finally, relative velocities in excess of ~ 1 m/s shatter aggregates into their constituent monomers. These laboratory results can be reconciled with numerical simulations by Dominik & Tielens (1997) if recently measured parameters governing rolling friction and binding energy are used (Blum & Wurm 2000).

Relative velocities between dust aggregates of less than ~ 1 m/s are certainly possible in protoplanetary disks (see Weidenschilling & Cuzzi 1993). However,

the actual velocity field of gas is neither strongly observationally constrained nor understood, given our perennial ignorance concerning sources of turbulence in protoplanetary disks. In a passive (non-turbulent) nebula, we expect relative velocities between similarly sized aggregates to grow with aggregate size, since larger particles achieve greater terminal velocities as they gravitationally settle towards the midplane. In the free molecular flow (Epstein) regime, the vertical terminal velocity in disks is of order

$$v_{\text{term}} \sim \sqrt{\frac{GM_*}{r^3} \frac{\rho_p a}{\rho_g}} \sim 4 \left(\frac{r}{\text{AU}} \right)^{9/7} \left(\frac{a}{1 \text{ cm}} \right) \text{ m/s}, \quad (3)$$

where M_* is the mass of the central star and G is the gravitational constant (see, e.g., CG97 or Youdin & Chiang 2003). We have assumed here that aggregates are sufficiently compact that they can be modelled as spheres. Then we might expect grains to attain terminal sizes of $\sim 1 (r/\text{AU})^{-9/7}$ cm, above which they would be moving so quickly as to shatter each other. Our simple estimate accords well with values cited in Blum & Wurm (2000) and Wurm, Blum, & Colwell (2001).⁶

3.3. Gravitational Instability

Gravitational forces between dust grains become important when their collective density exceeds the Roche density, $\sim M_*/r^3$. The original expectation was that such densities would eventually be achieved as dust settled towards the midplane into an ever thinner layer (Goldreich & Ward 1973). This hope was dashed for a period of several years after it was realized that Kelvin-Helmholtz turbulence generated within the particle layer prevented further settling of dust before Roche densities were attained (Cuzzi, Dobrovolskis, & Champney 1993; Weidenschilling 1995). The turbulence arises from vertical shear; dust-laden gas at the midplane rotates at nearly the full Keplerian velocity, while relatively dust-free gas residing above (and below) the midplane rotates more slowly as a consequence of radial pressure gradients that (usually) point outwards. Buffeted by the resultant Kelvin-Helmholtz turbulence, dust fails to attain densities greater than that of gas, falling short of the Roche density by 2 orders of magnitude.

Interest in gravitational instability has since been rekindled by Sekiya (1998) and Youdin & Shu (2002), who point out that the aforementioned turbulence can be overcome in disks having sufficiently super-solar metallicities. Turbulent eddies in gas can entrain only a finite amount of dust; the density of dust lifted to greater heights by turbulence cannot exceed the gas density. Whatever excess dust is not entrained must gravitationally precipitate out. Sekiya (1998) quantifies these ideas by calculating the density of dust as a function of height above the midplane in vertically shearing (Cartesian) flows that are marginally Kelvin-Helmholtz turbulent. Marginal turbulence means that the Richardson number at every point in the flow is assigned its critical value of 1/4 (see, e.g., Tritton 1988, p.350); dust is expected to settle to near this critical state. Sekiya

⁶See this latter work and the related chapter in this book for a proposal on how grain-grain sticking can exceed this maximum size.

(1998) finds that if the total, height-integrated dust-to-gas mass ratio (metallicity) exceeds the solar value by more than a factor of ~ 10 , then the dust density near the midplane becomes formally infinite. Youdin & Shu (2002) interpret the appearance of this singularity as the onset of gravitational instability.

How might super-solar metallicities be attained? Youdin & Shu (2002) discuss several metal enrichment processes, the simplest and most robust of which is aerodynamically induced, radial drift of solids. Solid particles encounter a headwind as they plow through sub-Keplerian gas; the resultant friction causes particles to be dragged radially inwards relative to gas. As particles migrate starward, they can “pile up” and generate local enhancements in the surface density of solids. Youdin & Chiang (2003) model this accretion process in detail, accounting not only for differences in the mean flow velocities between particles and gas, but also for the turbulent transport of angular momentum within the marginally Kelvin-Helmholtz unstable particle sheet, and the diminution of accretion velocities as the particle density approaches the gas density. They conclude that particle pile-ups are a robust outcome in protoplanetary disks; in a few $\times 10^5$ yr—timescales shorter than disk lifetimes of 10^7 yr—metallicity enhancements of more than a factor of ~ 10 can occur at stellocentric distances of several AU. A sample evolutionary sequence of surface density profiles is showcased in Figure 4.

Future work should follow the evolution of self-gravitating sheets of dust and calculate the size spectrum of resultant planetesimals.

3.4. A Cautionary Remark

Astrophysicists may wax eloquent on grain growth by gas-phase condensation, grain-grain collisions, and gravitational instability, but until they understand how chondritic meteorites are formed, it is possible that they are missing the boat. Chondritic meteorites are the oldest creations of the solar system; when we refer to the age of the solar system of 4.566 billion years, we are referring to the lead-lead ages of such meteorites. What has confounded meteoriticists and astrophysicists alike is why they contain nearly identically sized, once molten spheres, a.k.a *chondrules*, and their more refractory counterparts, *calcium-aluminum inclusions (CAIs)*. Their record-breaking ages, nearly solar composition, and enormous volume-filling fraction (50%–90% of the host meteorite) all suggest that these igneous, mm-to-cm-sized marbles are the building blocks of planetesimals; that to traverse the size ladder from microns to meters, one must necessarily melt and agglomerate chondrules first. Recently, Desch & Connolly (2002) have shown that the thermal histories of chondrules can be reproduced by processing of solid particles through strong hydrodynamic shocks having Mach numbers of 5–10 in the (possibly metallicity enhanced) solar nebula. The origin of such shocks, and the mechanism by which heated chondrules are collected into their host bodies with the observed high efficiencies, are unknown; see Chiang (2002) for a short review. Shocks are naturally generated by non-linear steepening of turbulent fluctuations within gravitationally unstable (Gammie 2001; Johnson & Gammie 2003) or magneto-rotationally unstable disks, though whether the requisite Mach numbers can be attained is unclear.

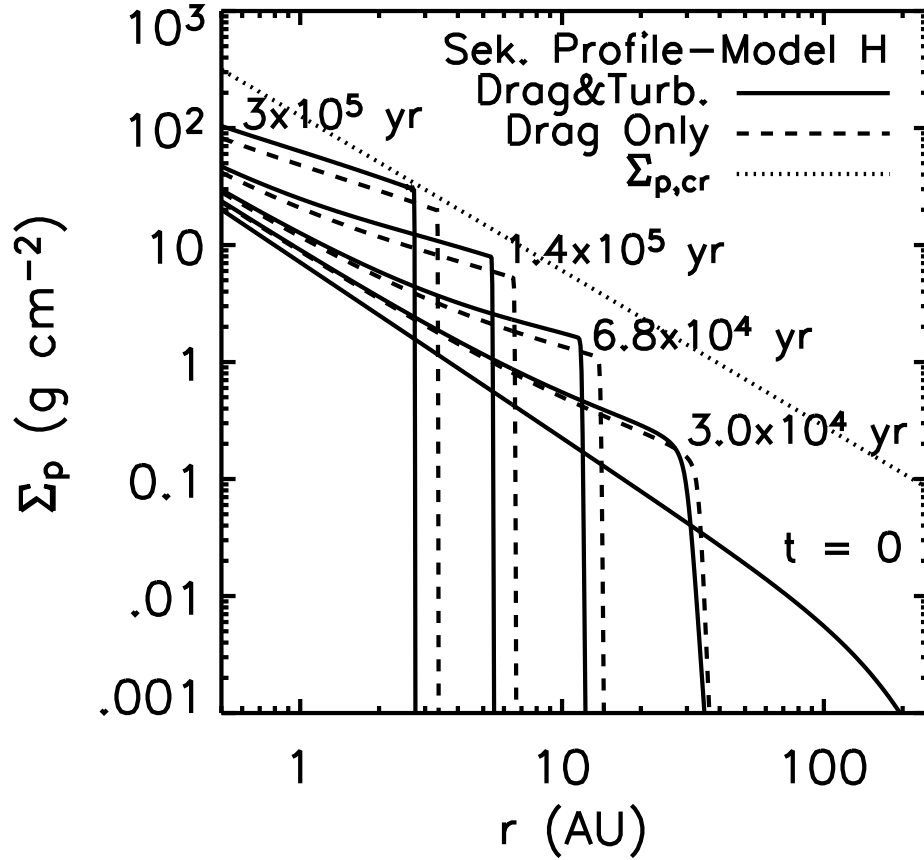


Figure 4. Evolution of the surface density of solids with time. Solids are modelled as millimeter-sized compact spheres. The particle disk shrinks and amplifies its surface density as it accretes inward by aerodynamic drag. Solid lines account for angular momentum transport by Kelvin-Helmholtz turbulence, which is seen to hasten the pile-up. At $t = 3 \times 10^5$ yr, the surface density at $r \sim 3$ AU exceeds the critical threshold (dotted line) above which gravitational instability is thought to occur. Figure taken from Youdin & Chiang (2003).

4. Dusty Signposts of Planets

Young planets can leave their mark on the reservoirs of dust from which they arose by gravitationally torquing dust into signature non-axisymmetric patterns. The phenomenon is well studied in the solar system context; for example, Kuiper belt objects (read: very large dust particles) that inhabit the exterior 3:2 mean-motion resonance with Neptune preferentially attain perihelia at longitudes displaced $\pm 90^\circ$ away from that planet. An instantaneous snapshot of thousands of 3:2 resonant objects would reveal a characteristic “keyhole” pattern that rotates with the angular speed of Neptune; see Figure 5, taken from Chiang & Jordan (2002).

Observations of similar non-axisymmetric patterns of dust surrounding other stars are used to implicate the existence of planets. Thermal emission at sub-mm wavelengths is spatially resolved around the stars ϵ Eridani (Ozernoy et al. 2000), Fomalhaut (Holland et al. 2003), and Vega (Wilner et al. 2002). Around each star are several clumps of emission interpreted to arise from dust particles trapped in mean-motion resonances with an as yet unseen planet. The dust particles are hypothesized to be generated from the collisions of yet larger planetesimals; Poynting-Robertson drag brings the dust into mean-motion resonance, where they resonantly librate for a spell, and eventually brings them out again. In the case of Vega, two clumps of emission are detected at a projected stellocentric distance of ~ 80 AU, and appear nearly diametrically opposed. Ascribing these clumps to be the limb-brightened edges of a circumstellar ring viewed edge-on is not the most natural interpretation, since Vega the star is thought to be viewed nearly pole-on (Gulliver et al. 1994). The clumps are alternatively interpreted as dust particles temporarily trapped in $n:1$ resonance with a Jovian-mass planet on a highly eccentric orbit having a semi-major axis of 40 AU, where n can be an integer greater than 3 (Wilner et al. 2002; Kuchner & Holman 2002). While the parameters of the planet—e.g., the mass and orbital eccentricity—can not be pinned down with great accuracy, and while there is concern as to whether interparticle collisions might vaporize dust en route to resonance trapping, the scenario at least has a robust, testable prediction: the clumps should rotate on the sky with a pattern speed that is not equal to the local Keplerian frequency, but is rather equal to half the mean orbital frequency of the planet (Kuchner & Holman 2002). The magnitude of the expected pattern speed is sufficiently large in the case of Vega— $1^\circ/\text{yr}$ —that multi-epoch observations should be able to test this prediction.

Acknowledgments. Support for this work was provided by Hubble Space Telescope Theory grant HST-AR-09514.01-A. We thank the organizers for a highly instructive conference.

References

- Beckwith, S.V.W., Sargent, A.I., Chini, R.S., & Güsten, R. 1990, *AJ*, 99, 924
 Beckwith, S.V.W., & Sargent, A.I. 1991, *ApJ*, 381, 250

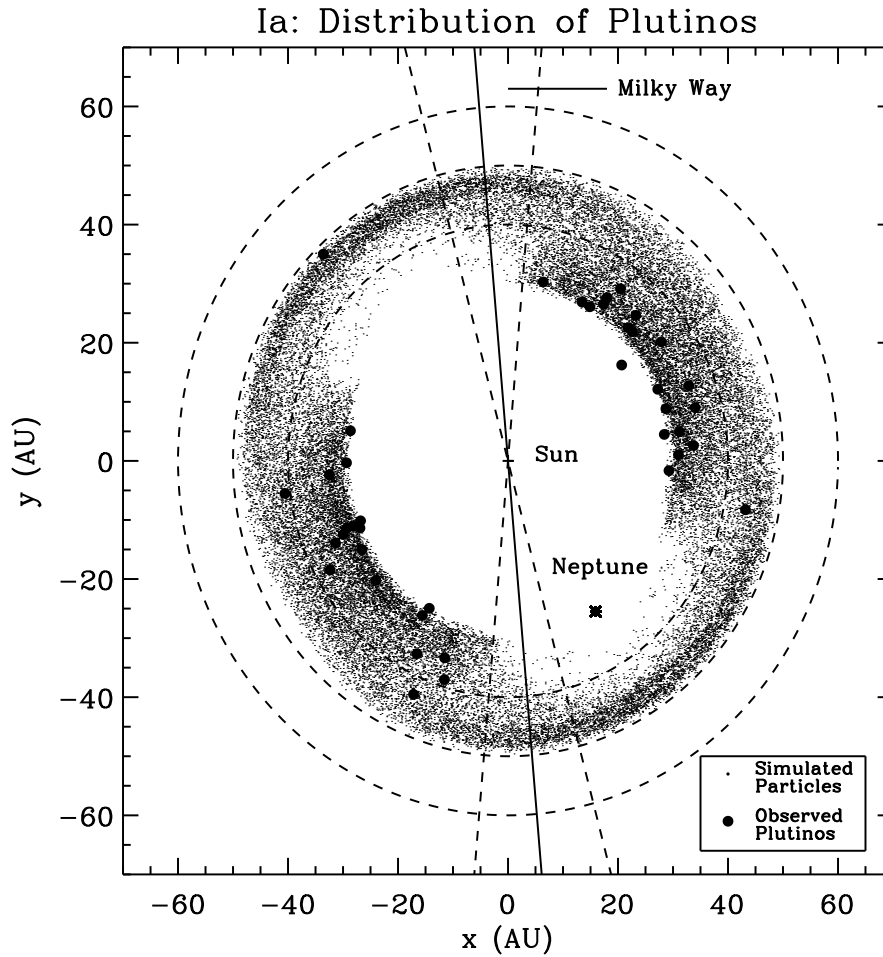


Figure 5. Theoretical snapshot, viewed above the plane of the solar system, of the spatial distribution of Kuiper belt objects that are 3:2 resonant with Neptune. The clumping of objects $\pm 90^\circ$ from Neptune's position follows from the shape of the resonant perturbation potential established by Neptune, not from the self-gravity of Kuiper belt objects. The entire keyhole-like pattern rotates with the angular speed of Neptune. Dashed circles indicate heliocentric distance of 40, 50, and 60 AU. Solid circles denote positions of known 3:2 resonant objects (also called "Plutinos.") Similar patterns might be traced out by dust particles in resonance with extrasolar planets. Figure taken from Chiang & Jordan (2002).

- Beckwith, S.V.W., Henning, T., & Nakagawa, Y. 2000, in *Protostars and Planets IV*, eds. V. Mannings, A.P. Boss, and S.S. Russell (Tucson: University of Arizona Press), 533–558
- Blum, J., & Wurm, G. 2000, *Icarus*, 143, 138
- Bohren, C.F., & Huffman, D.R. 1983, *Absorption and Scattering of Light by Small Particles* (New York: Wiley), p.72
- Calvet, N., Patiño, A., Magris, G., & D’Alessio, P. 1991, *ApJ*, 380, 617
- Calvet, N., et al. 2002, *ApJ*, 568, 1008
- Chiang, E.I., 2002, *Meteoritics and Planetary Science*, 37, 2 (astro-ph:/0205274)
- Chiang, E.I., & Goldreich, P. 1997, *ApJ*, 490, 368 (CG97)
- Chiang, E.I., & Jordan, A.B. 2002, *AJ*, 124, 3430
- Chiang, E.I., et al. 2001, *ApJ*, 547, 1077 (C01)
- Cotera, A.S., et al. 2001, *ApJ*, 556, 958
- Cuzzi, J.N., Dobrovolskis, A.R., & Champney, J.M. 1993, *Icarus*, 106, 102
- D’Alessio, P., Cantó, J., Calvet, N., & Lizano, S. 1998, *ApJ*, 500, 411
- Dominik, C., & Tielens, A.G.G.M. 1997, *ApJ*, 480, 647
- Dullemond, C.P., van Zadelhoff, G.J., & Natta, A. 2001, *ApJ*, 389, 464
- Dullemond, C.P., Dominik, C., & Natta, A. 2001, *ApJ*, 560, 957
- Gammie, C.F. 2001, *ApJ*, 553, 174
- Goldreich, P., & Ward, W.R. 1973, *ApJ*, 183, 1051
- Gulliver, A.F., Hill, G., & Adelman, S.J. 1994, *ApJ*, 429, L81
- Henning, Th., & Stognienko, R. 1996, *A & A*, 311, 291
- Holland, W.S., et al. 2003, *ApJ*, 582, 1141
- Johnson, B.M., & Gammie, C.F. 2003, *ApJ*, submitted.
- Koerner, D.W., Chandler, C.J., & Sargent, A.I. 1995, *ApJ*, 452, L69
- Kuchner, M.J., & Holman, M.J. 2003, *ApJ*, 588, 1110
- Malfait, K., et al. 1998, *A & A*, 332, L25
- McCabe, C., Duchêne, G., & Ghez, A.M. 2003, *ApJ*, 588, L113
- Natta, A., Meyer, M. R., & Beckwith, S. V. W. 2000, *ApJ*, 534, 838
- Ozernoy, L.M., et al. 2000, *ApJ*, 537, L147
- Sekiya, M. 1998, *Icarus*, 133, 298
- Tritton, D.J. 1988, *Physical Fluid Dynamics* (Oxford: Clarendon Press), p350–357
- van Boekel, R., et al. 2003, *A&A*, 400, L21
- Weidenschilling, S.J. 1995, *Icarus*, 116, 433
- Weidenschilling, S.J., & Cuzzi J.N. 1993, in *Protostars and Planets III*, eds. E.H. Levy and J.I. Lunine (Tucson: University of Arizona Press), 1031–1060
- Weinberger, A.J., et al. 2002, *ApJ*, 566, 409
- Wilner, D.J., et al. 2002, *ApJ*, 569, L115
- Wood, K., Wolff, M.J., Bjorkman, J.E., & Whitney, B. 2002, *ApJ*, 564, 887
- Wurm, G. & Blum, J. 1998, *Icarus*, 132, 125
- Wurm, G., Blum, J., & Colwell, J.E. 2001, *Icarus*, 151, 318

Youdin, A.N., & Chiang, E.I. 2003, ApJ, submitted.

Youdin, A.N., & Shu, F.H. 2002, ApJ, 580, 494